# A MEASUREMENT OF THE SKY BRIGHTNESS TEMPERATURE AT 408 MHz

By R. M. Price*

### Summary

The absolute value of the background brightness temperature has been measured at a radiofrequency of 408 MHz. Observations were made with a large pyramidal "standard gain" horn aerial and the aerial temperatures were compared direct with the temperature observed with the receiver input connected to a matched resistive load of known temperature. For the region within 24° of the south celestial pole an average brightness temperature of 23·9°K was obtained. Observations of northern regions indicate that values from previous determinations at northern latitudes are 4–5 degK too high.

## I. INTRODUCTION

Absolute values of the brightness temperature of the background radio emission are of interest in a number of different astronomical problems. For example, absolute values provide a reference level for determination of the percentages of linear polarization observed in the background radiation at decimetre wavelengths. These percentages are necessary in the interpretation of the relationships between highly polarized regions of the background and the structure of nearby emitting regions within the disk of the Galaxy. Absolute measurements at a number of frequencies can give the value and form of the spectral index of the background radiation from different regions of the Galaxy. Such results will relate direct to the question of large-scale structure of the magnetic fields and the distribution of relativistic electrons in the Galaxy. Finally, it is necessary to know absolute levels in order to predict the form of the $(\log N)-(\log S)$ relationship and to determine the radio luminosity function for radio sources. Since many of the above problems have been investigated using data obtained near 408 MHz this frequency was chosen for the present investigation.

In northern latitudes several measurements of the value of the sky brightness near 400 MHz have been made previously (Seeger, Stumpers, and van Hurch 1960, further refined by Seeger *et al.* 1965—hereafter referred to as SWCH; Pauliny-Toth and Shakeshaft 1962—hereafter referred to as PTS). These studies used the north celestial polar region as a primary reference region. For the southern sky, one estimate of the background brightness temperature has been made by McGee, Slee, and Stanley (1955) which applied to the cold region near right ascension $04^h 30^m$, declination $-34°$.

* Department of Astronomy, Research School of Physical Sciences, Australian National University, Canberra, A.C.T. 2600; present address: Department of Physics and Research Laboratory of Electronics, Massachusetts Institute of Technology, Cambridge, Massachusetts, U.S.A.

The present measurements were undertaken at the Australian National Radio Astronomy Observatory to establish a baselevel for use in the southern hemisphere and to determine the accuracy and consistency of the previous measurements of PTS which have been adopted as a standard by northern hemisphere observers. The south celestial pole was used as the primary reference region in this study. Two additional regions near the equator were observed for comparison with the PTS results.

## II. Principles of the Measurement

The measurement consists essentially of the comparison of the output of a receiver when connected in turn to a standard gain aerial and to matched loads of known temperatures. In practice, it is necessary to compare the aerial output with that of a load at only one temperature, as long as the temperature scale factor at the output of the receiver is known and the receiver is linear over the range of the measurements. The scale factor is easily established by use of a reference noise signal which can be separately calibrated in terms of a matched load at two or more known temperatures.

In order to discuss the corrections which must be made to the observed aerial temperature it is necessary to define the power response of the horn antenna. The definitions given here follow Seeger, Westerhout, and van de Hulst (1956), with the exception of the definition of the full beam response. For the present investigation the response out to 24° from the beam axis in both the $E$ plane and $H$ plane is taken. This value was chosen as the boundary for the full beam, since the power response in the two planes is equal at this point and is just above the level where the second $E$ plane side lobe is found. The remaining definitions are as follows: $A(\theta, \phi)$ is the aerial power response function over the sphere with the aerial at its centre; $A(\theta_0, \phi_0)$ is normalized to unity along the beam axis in the forward direction; $\theta$ is the angular distance from the beam axis and $\phi$ is the angular measure in the plane normal to the beam axis and containing the aerial.

The total beam response $\Omega$ is the total power response of the aerial over the entire sphere and is given by the integral

$$\Omega = \iint_{4\pi} A(\theta, \phi) \sin \theta \, d\theta \, d\phi \,. \tag{1}$$

The full beam response $\Omega'$ is the power response integrated over the area previously defined as the full beam, i.e. out to $\theta = 24°$ for all values of $\phi$:

$$\Omega' = \int_0^{2\pi} \int_0^{2\pi/15} A(\theta, \phi) \sin \theta \, d\theta \, d\phi \,. \tag{2}$$

The geometrical area of the aerial is simply given by the dimensions of the aperture

$$A_{\mathrm{g}} = ab \,.$$

The effective area is given by the formula

$$A_e = (\lambda^2/4\pi)G,$$

where $G$ is the forward gain of the aerial and is found from calculations (see Section III).

To estimate the contribution to the aerial temperature from power incident outside the full beam it is necessary to evaluate the integral

$$\Omega^{-1} \int_{2\pi/15}^{\pi} \int_{0}^{2\pi} A(\theta, \phi) \, T_t(\theta, \phi) \sin \theta \, d\theta \, d\phi, \tag{3}$$

where $T_t(\theta, \phi)$ is the distribution of the brightness temperature over the sphere, at the time $t$ of the measurement, whether it be sky or ground contribution. This integral cannot be solved analytically and an approximate numerical solution must be made. Such a solution involves the summation

$$\sum_i \sum_j A(\theta_i, \phi_j) \, T_t(\theta_i, \phi_j),$$

where $T_t(\theta_i, \phi_j)$ is the brightness temperature in a given direction at the time of observation and $A(\theta_i, \phi_j)$ is the response of the aerial in the same direction.

The estimation of this summation is made possible by the measurement of the aerial response away from the main beam and a knowledge of the approximate brightness temperature distribution over the sky at the time of the measurement of aerial temperature. These factors are discussed in further detail in Section V.

From the above discussion it can be seen that the measured aerial temperature $T_a$ does not directly represent the brightness temperature of the region of the sky to which the aerial beam is directed. To obtain this true brightness temperature, $T_a$ must first be corrected for losses in the aerial and feed lines up to the point of the receiver input. The effective temperature as measured at the receiver input is then given by

$$T_a = T_a'(1-\alpha) + \alpha T_0, \tag{4}$$

where $T_a'$ is the aerial temperature of an equivalent loss-free antenna, $\alpha$ is the loss factor for the horn antenna and feed sections, and $T_0$ is the ambient temperature of the antenna and feed. $T_a$ can then be separated into the following temperature components: $T_{fb}$ contributed from regions of the sky within the full beam of the aerial, $T_g$ contributed from ground radiation, $T_s$ contributed from regions of the sky outside the full beam. It follows that

$$T_a' = T_{fb} + T_g + T_s. \tag{5}$$

Finally, $T_{fb}$ consists of a contribution from the average brightness temperature $T_b$ of the region of the sky within the full beam of the aerial, and $T_{atm}$, a contribution

due to the emission of the atmosphere. Thus, if $X$ is the fraction of the total power received by the aerial which is in the full beam, the average brightness temperature within the full beam is given by

$$\bar{T}_b = T_{fb}/X - T_{atm}. \qquad (6)$$

### III. Equipment

#### (a) Aerial

A pyramidal horn aerial was chosen for the present investigation. Such an aerial has the advantage that its forward gain and main beam response can be accurately calculated from knowledge of the dimensions of the aperture and the field distribution across the aperture.

The ease with which the horn could be mounted and steered limited the length to approximately 8 m or about 10 wavelengths at the observing frequency of 408 MHz. The forward gain obtained with a horn of this length is approximately 22 dB. With the use of the methods outlined in Silver (1949), Slayton (1954), and Braun (1956), the following sizes were calculated for the horn aerial:

aperture       $E$ plane   4·50 wavelengths,      $H$ plane   6·10 wavelengths;

length (aperture to throat)      8·98 wavelengths.

This design gave a slightly elliptical beam at the half-power points ($E$ plane, 12°·5; $H$ plane, 14°) at 408 MHz. The calculated forward gain was 22·1 dB, referred to an isotropic radiator. Such calculations have been shown by experiment to be accurate to $\pm 2 \cdot 5°$ (Jull and Deloli 1964).

The horn was constructed at Parkes, N.S.W. The frame was made of light steel tubing, and the conducting surface inside the frame was $14 \times 18$(wires per inch) $\times 33$ gauge bronze mesh. All seams were continuously soldered to ensure good electrical conductivity. At the throat and aperture of the horn the mesh was secured by a brass strip screwed to the frame.

The transit mount on which the horn rested was a dual A-frame type which allowed the horn to be pointed at any altitude along the meridian. The horn could be locked in position at intervals of 2·5° of altitude over its entire range of movement.

*Ground screen.* All the ground within 10 m of the horn and mounting was covered with a 2 in. chicken wire mesh to prevent ground radiation entering the back and distant side lobes of the aerial that might "see" the ground. North of the horn at distances of 15 and 35 m, fences $2\frac{1}{2}$ m high were erected. These extended approximately 20 m either side of the north–south line through the horn and helped minimize the amount of ground radiation entering the back lobes of the horn when it was pointed at the south celestial pole, the primary reference region.

*Waveguide section and coaxial transition.* The waveguide section was a standard size for the frequency range. Its dimensions were 26·27 cm in the $E$ plane by 53·34 cm in the $H$ plane. The section was of all brass construction to ensure good conductivity. The section supported only the $TE_{01}$ mode of propagation at 408 MHz.

A crossbar coaxial-to-waveguide transition was used to couple the waveguide section to the receiver input. The crossbar transition was chosen because of its broadband matching properties.

The crossbar and probe were placed about 50 cm back from the throat of the horn, this distance being sufficient for any higher modes produced by the crossbar to evanesce before reaching the horn where they might propagate.

### (b) Receiver System

The receiver system used for the investigation was a switched, crystal-mixer-type radiometer. The receiver accepted both the signal and image sidebands, each of 10 MHz bandwidth, extending from 4 to 14 MHz. The measured system temperature was 350°K and, with an output time constant of 2 sec, peak-to-peak fluctuations were measured to be equivalent to 0·7 degK of aerial temperature.
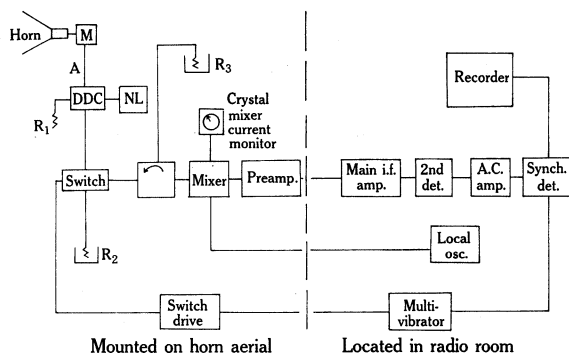


Fig. 1.—Block diagram of receiver used in measurement:
M,      matching section
A,      receiver input
DDC,  dual directional coupler
NL,    noise lamp
C,      circulator

A block diagram of the receiver is shown in Figure 1. The coaxial matching section M was considered as part of the aerial system, and the receiver input A was at the input of the dual directional coupler DDC. The directional coupler allowed a calibration from an argon discharge noise tube to be injected into the receiver.

The coaxial diode switch alternately connected the mixer input to signal and reference arms of the switch. The termination on the reference side of the switch was immersed in liquid nitrogen. The switch was isolated from the mixer by means of a three-port circulator. The third port of this circulator was also terminated in a matched load immersed in liquid nitrogen. Any excess noise generated in the mixer crystal or noise reflected from the mixer input could not propagate back toward the receiver input but was absorbed in the load on the circulator. This third port also provided a facility for injecting a high-level noise signal to investigate the reflection coefficient or mismatch of the components on either arm of the switch.

The switch, circulator, mixer, and i.f. preamplifier were located at the horn aerial to minimize transmission line losses. The back end of the receiver system was in a small building 15 m from the aerial.

## IV. System Measurements

### (a) Match

The reflection coefficient, or standing wave ratio (swr) of both the horn and comparison termination, was measured by the conventional means of a signal generator, slotted line, and detector. For the aerial a vswr of better than 1·1 was achieved

over the frequency range 380–430 MHz.  The termination had similar vswr over the same frequency range.  It was important, however, to know the actual swr at the input to the receiver under operating conditions with the horn or reference termination connected.  This measurement was made possible by the use of the circulator.  With the system in its normal operating state, a high-level noise signal from an argon discharge was introduced through the circulator, propagating from the receiver toward either the horn or the reference termination on the input.  If a mismatch existed, a fraction of the noise signal power was reflected back to the receiver where it was detected, as if it had been power delivered from the respective element.  The matching device at the receiver input was then adjusted until the reflected power reached a minimum, indicating that the best possible match, under the conditions present, had been achieved.

This method has several obvious advantages.  Firstly, it allows *in situ* measurements of the match at the receiver input; secondly, it uses the full sensitivity of the receiver system as a detector and allows a high degree of precision in the measurement of the reflected power; and finally, it is independent of the band-pass characteristics of the receiver since the same band-pass operates in all of the tests.

### (b) Losses

To determine the loss in the coaxial matching section used on the horn aerial, one end was short circuited and the vswr at 408 MHz was measured.  If the loss is assumed to be purely a distributed resistive loss, it is related to the measured vswr by the relationship

$$\alpha = 10 \log_{10}\{(\text{vswr}+1)/(\text{vswr}-1)\} \quad \text{dB}. \tag{7}$$

The test on the matching section yielded a vswr of $70\pm4$, which indicated a loss of $0\cdot124\pm0\cdot006$ dB.

With the end of the waveguide transition section shorted by a sheet of brass clamped securely to the flange, the vswr at the waveguide–coaxial output was measured as $147\pm6$, corresponding to a loss of $0\cdot058\pm0\cdot002$ dB.

An estimate of the losses in the horn by treating it as a section of waveguide of increasing cross section yielded a loss of approximately $0\cdot01$ dB, and this value was adopted in subsequent calculations.

The losses in the comparison termination and its matching stub were found by substituting a short circuit for the resistive element and subsequently measuring the vswr.  This yielded a value of $29\cdot2\pm1\cdot0$ for the load and its tuning stub.  The corresponding loss is $0\cdot30\pm0\cdot01$ dB.

Since the comparison termination is substituted for the aerial system at the receiver input, losses in the remaining radiofrequency components need not be known.  They are common to both the signal and reference measurements and serve only to increase slightly the effective noise temperature of the receiver system.

### (c) Beam Pattern Tests

With the use of edge diffraction theory the entire beam response of a horn aerial can be calculated.  However, experimentally it is found that for side and back lobes the difference between the calculated and measured responses can become

large. This difference can arise from a number of sources, e.g. mechanical imperfections in the horn aperture, ohmic losses in the walls of the horn, currents on the outside of the horn walls, and higher order modes present at the horn aperture. Any of these effects can cause a difference between the field distribution at the aperture of the actual horn and that at the mouth of the theoretical radiator, resulting in a beam response different from the calculated one.

Accurate knowledge of the beam response can only be derived from measurements on the actual horn aerial under operating conditions. For these measurements an aerial test range was set up. The transmitting aerial, a pyramidal horn with aperture dimensions 60 cm by 60 cm was situated on top of a 12 m tower which could
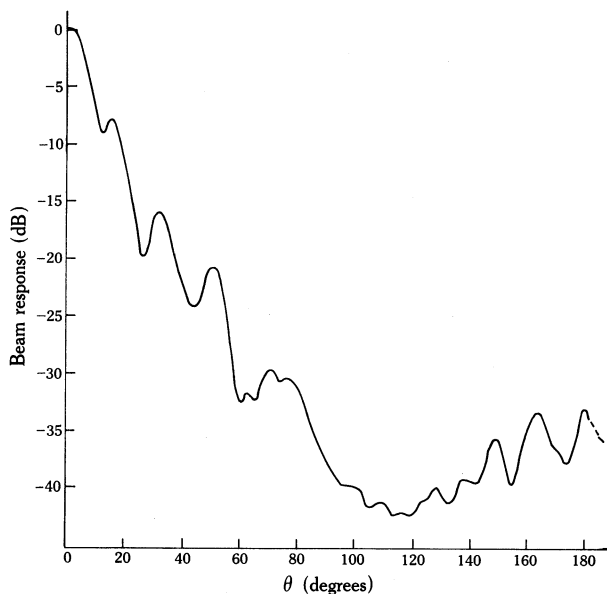


Fig. 2.—Measured power response pattern of the horn aerial in its $E$ plane. The response in decibels below that in the forward direction is plotted against $\theta$, the angular distance from the forward horn axis in the $E$ plane.

be moved along a north–south line, therefore on the $E$ plane axis of the horn. Two fences, each $2\frac{1}{2}$ m high, between the horn aerial under test and the transmitter, prevented ground reflections. As the horn aerial was moved along the meridian, its response in the $E$ plane was measured. The transmitted power was varied to keep the receiver output at a constant level as the direction in which the horn was pointed was changed. The transmitted power required to obtain the given receiver output was then a measure of the response of the aerial in that direction.

The response was derived with the transmitting tower in three different positions: 45, 90, and 150 m distant from the horn aerial on a north–south line. The results of these tests are shown in Figure 2.

Since it was not possible to move the horn aerial in azimuth and very difficult to move the transmitting tower on a circle of constant distance from the horn, the $H$ plane pattern was measured by observations of the Sun. These measurements

did not allow the $H$ plane pattern to be plotted below $-20$ dB, where owing to side lobe structure, variations in the background are larger than the expected response.

Another method which has been successfully applied in the determination of the response of horn aerials is the use of scaled aerials. Experimentally it is found that aerials with the same dimensions in wavelengths have identical beam responses. This fact allowed the comparison of the horn used in the present experiment with similar standard gain horns developed by the Naval Research Laboratory (Slayton 1954). The NRL $3 \cdot 2$ cm horn has the same aperture dimensions $(4 \cdot 50\lambda \times 6 \cdot 08\lambda)$ and the same gain as the present horn. The calculated and measured gains of the NRL horn were identical, $22 \cdot 1$ dB, with a dispersion of $0 \cdot 1$ dB in the gain measurements. The NRL horn beam response in the $H$ plane was determined to a level of $-32$ dB, the limit of sensitivity, and this result was used where applicable to determine corrections for radiation received from outside the full beam of the horn in the present investigation.

### (d) Effective Temperature of Substitution Load

The effective temperature of the substitution load was calculated from knowledge of the temperature of the resistive element, losses in the coaxial transmission section, and the temperature gradient along the transmission section. The loss in the load and tuning stub, noted previously, was $0 \cdot 30 \pm 0 \cdot 01$ dB.

When the resistive element was immersed in liquid nitrogen, the contribution of the losses became evident, as much of the load and matching stub remained at ambient temperature. The boiling point of liquid nitrogen is $77 \cdot 3°\text{K}$; this can be increased by as much as $0 \cdot 2$ degK for up to $2\%$ dissolved oxygen. In the present experiment it was calculated to be approximately $0 \cdot 5$ degK lower, considering the atmospheric pressure at the time of the observations. The effective temperature of the nitrogen was taken as $77 \cdot 0 \pm 0 \cdot 5°\text{K}$.

The resistive element of the termination was in good thermal contact with the nitrogen. However, if it were not in thermal equilibrium with the nitrogen, its temperature might have been expected to be slightly higher. It is estimated that error from this source did not exceed $0 \cdot 5$ degK.

Following Stelzried (1961) the effective noise temperature of the load, i.e. the resistive termination and the associated coaxial transmission line, was calculated by dividing the line into four sections, each with a loss $\alpha_i$ and an average temperature $T_i$. The assigned lengths of the sections were determined from the following measurements: the length of the line below the surface of the liquid nitrogen, the length above the surface of the nitrogen where ice formed on the line, and the remainder of the load to the output connector. The matching stub was then considered as an additional section.

The average temperature was estimated for each section and the losses were calculated on the assumption that the measured losses were evenly distributed over the length of the coaxial transmission line. With these quantities, the effective noise temperature of the load is given by

$$T_\text{L} = \alpha_\text{s} T_\text{s} + \alpha_3 t_\text{s} T_3 + \alpha_2 t_3 t_\text{s} T_2 + \alpha_1 t_2 t_3 t_\text{s} T_1 + t_1 t_2 t_3 t_\text{s} T_\text{re},$$

where $t_i = (1-\alpha_i)$ is the transmission coefficient for the $i$th section, and the subscripts s and re indicate the stub and resistive elements respectively.

From this equation the effective temperature of the load presented at the receiver input when immersed in liquid nitrogen was calculated to be $88 \cdot 1 \pm 0 \cdot 7°$K. The effective temperature with the load immersed in ice water was calculated to be $273 \cdot 6 \pm 0 \cdot 2°$K.

### (e) Calibration of Noise Lamp Signal

For an accurate comparison of the difference in the aerial temperature between the horn and the reference termination, it was necessary to know the magnitude of the signal introduced by the argon discharge noise lamp. This signal was used to establish the output scale factor for given temperatures at the receiver input.

To determine the value of the noise lamp the following procedure was used. The reference termination was immersed in ice water and connected to the receiver input. The match was adjusted to give the minimum vswr over the receiver bandpass. The noise lamp was then turned on and the increase in receiver output noted. With the noise lamp once again turned off, the reference termination was immersed in liquid nitrogen. After the receiver output reached its new level, giving a constant output, it was assumed that the termination had reached the temperature of the liquid nitrogen.

The match of the termination was again tested to ensure that it had remained the same. The noise lamp calibration signal was again switched on and the increase in receiver output noted. (This also provided a test of the linearity of the detector law over the range of the measurements.) The difference in levels between the receiver output with the termination in ice water and liquid nitrogen after correction for detector law established the temperature scale for the receiver output. The value of the noise lamp calibration signal in terms of aerial temperature could then be obtained. The derived value for the signal was $61 \cdot 5 \pm 1 \cdot 0°$K.

## V. CORRECTIONS TO AERIAL TEMPERATURE

Corrections must be made to the measured aerial temperature for the contribution of the power received in the side and back lobes of the horn aerial. These corrections are difficult to determine and have been the main source of error in some previous measurements of the background brightness temperature. The corrections made to the present measurements allow for ground radiation, the sky contribution outside the full beam of the aerial, and the atmospheric contribution to the full beam temperature.

### (a) Ground Radiation $T_g$

As the horn mounting did not allow movement in azimuth, it was not possible to use the standard technique of tracking a given region of the sky over a large range of hour angle to determine the zenith angle effects (such effects being due primarily to the variation of ground radiation with zenith angle). The method used was to compare the apparent brightness temperature of regions at upper and lower culmination. Because of the large zenith angle of the south celestial pole (57°) from the observing site, it was possible to make such measurements only for zenith angles

24° to 90° south. These measurements of the difference in brightness temperature at upper and lower culmination were then fitted to a model, considering the shape of the beam "seeing" the ground at a given zenith angle. The variation of ground contribution with zenith angle derived is shown in Figure 3.

From the measurements of the beam response and numerical evaluation of equation (3) it was found that approximately 5% of the total power accepted by the aerial was from regions with $\theta > 90°$, that is, from the back hemisphere. On this basis, taking the ground as being at ambient temperature at vertical incidence, and approximately 100°K at grazing incidence (derived from the zenith angle tests), the total contribution to be expected from the ground with the aerial pointed toward the zenith is $T_g = 9°K$.
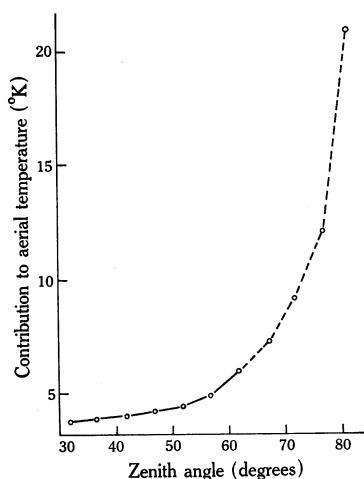


Fig. 3.—Zenith angle effects determined by comparison of measurements of selected southern regions at upper and lower culmination. Determination of the baselevel at zenith angle 0° is discussed in the text.

At zenith angle 57° south (the south celestial pole) the calculated ground contribution rises to 9·6°K without the ground screen, the increase of 0·6 degK being comparable with the value indicated from the zenith angle tests. With the ground screen in place around the aerial, the calculated ground contribution at zenith angle 57° drops to 4·9°K.

### (b) *Sky Contribution Outside Full Beam* $T_s$

The average brightness temperature over the sky visible at the time of the observations of the south celestial pole was estimated from the brightness distributions shown by the survey of McGee, Slee, and Stanley (1955) at 400 MHz and Piddington and Trent (1956) at 600 MHz. The results of these surveys were scaled and adjusted to the base values determined by Pauliny-Toth and Shakeshaft (1962) at 404 MHz in the northern sky. On this basis, the average brightness temperature of the sky visible during the several observing periods was estimated to vary between 37°K and 41°K.

The value of $T_s$ derived from these average brightness temperatures is then subtracted from the measured aerial temperature according to equation (5). If the final brightness temperature obtained indicates an error in the baselevel adopted

from Pauliny-Toth and Shakeshaft, a new value for the baselevel will be applied, entering the final result as a second-order correction.

Considering the power response outside the full beam, the calculated contribution from the sky was $4 \cdot 4°$K when the aerial was pointed at the south celestial pole. The uncertainty in the average brightness temperature over the sky introduces a possible error of $\pm 0 \cdot 5$ degK in the sky contribution to the total observed aerial temperature.

### (c) *Atmospheric Contribution* $T_{atm}$

From curves published by Hogg (1959) the approximate contribution to the sky temperature to be expected from the atmosphere at 408 MHz is 1 degK at the zenith. This contribution is included in the calculated sky contribution $T_s$ and is allowed for in the final calculations of full beam brightness temperature outside the atmosphere. For a simple secant extinction relationship, the contribution of the atmosphere at zenith angle 57° is approximately $1 \cdot 8$ degK.

## VI. Observations

The primary reference region chosen for the determination of the absolute sky brightness temperature in this investigation was the region centred on the south celestial pole. Its constant position in the sky makes it an obvious choice for such a standard region. Measurements were also made of regions near the celestial equator at $\alpha = 14^h 50^m$, $\delta = -5°$ and $\alpha = 22^h 00^m$, $\delta = +5°$.

For the standard region measurements the aerial was pointed direct at the south celestial pole and the receiver output noted. The match of the horn at the receiver input was measured and the amplitude of the noise lamp calibration signal was recorded. The reference termination was then substituted for the horn aerial at the receiver input and the match adjusted to ensure that it was the same as that of the horn. The substitution was made both with the termination at ice and liquid nitrogen temperatures to provide two reference points. The amplitude of the noise lamp signal was noted with the reference load at both temperatures to check that the receiver was not overloaded and that the detector characteristic was linear. The comparison between the cold load and the aerial was made a number of times each night of the observations.

The observations were carried out in the interval $20^h$–$00^h$–$03^h$ local solar time. There was no nearby automobile traffic at this time, and other possible sources of interference, such as electrical machines, were thought to be at a minimum. In an attempt to detect any interference, the local oscillator of the receiver system was tuned through several megahertz and the i.f. noise of the receiver was monitored on a cathode ray oscilloscope. No interference was noted at any time during the observations. In addition, the nature of the i.f. noise was found to be the same for the load, which is not susceptible to external r.f. interference, and the aerial.

It was found that the receiver output with the aerial pointed at the south celestial pole exhibited a small systematic variation with a period of 12 hr. This variation, measured to be $0 \cdot 5$ degK of aerial temperature, was due to the asymmetry of the aerial response in the $E$ plane and $H$ plane away from the main lobe. As the

brighter regions toward the Magellanic Clouds and the plane of the Galaxy came into the broader $E$ plane, the receiver output was noted to rise. Calculations of the expected sky contribution to the aerial temperature indicated that a change of $0 \cdot 6$ degK was to be expected. This variation was accounted for in the correction for the sky contribution $T_s$ in the calculation of the final brightness temperature.

## VII. RESULTS

### (a) South Celestial Pole Region

The aerial temperature measured at the receiver input while the aerial was pointed at the south celestial pole was $41 \cdot 0°K$. Correcting this for contributions from the loss in the aerial and matching section according to equation (4), with $\alpha = 0 \cdot 041$ dB, $(1-\alpha) = 0 \cdot 959$, and $T_0 = 283°K$

$$T'_a = (T_a - \alpha T_0)/(1-\alpha) = 30 \cdot 7°K \,.$$

Then, combining equations (5) and (6),

$$\bar{T}_b = (T'_a - T_g - T_s)/X - T_{atm} \,,$$

with

$$T_g = 4 \cdot 9°K \,, \qquad T_s = 4 \cdot 4°K \,, \qquad T_{atm} = 1 \cdot 8°K \,,$$

as derived in the previous section.

The fraction of the power in the full beam is calculated from integration of the beam response over the full beam, $\Omega'$, and over the entire sphere, $\Omega$. The fraction $X$ of the power in the full beam is then given by

$$X = \Omega'/\Omega = 0 \cdot 85 \,.$$

Therefore to first order the average brightness temperature of the region of the sky centred on the south celestial pole and included in the full beam of the horn aerial is $23 \cdot 4°K$. This is the brightness temperature which would be observed by a loss-free aerial with all of its power in the full beam and looking through a loss-free atmosphere at the south celestial pole. This result is subject to second-order corrections which are discussed in Subsection (c).

### (b) Northern Reference Regions

The temperature determinations in the northern regions were more uncertain than those at the south celestial pole. Since the aerial could not track the regions, the observations had to be carried out in a short period of time and only a small number of substitutions were possible. The determination of the baseline stability of the receiver system over such periods was also less certain. Observations of the northern regions were carried out by substitution of the reference load at 0°C only. The expected errors from gain variations and nonlinearities in the receiver system over this large temperature range are therefore greater. In order to obtain some idea of the accuracy to be expected from the measurements over this temperature range, measurements of the south celestial pole were carried out under the same conditions

during the same observing sessions. They indicated that the standard deviation of the seven substitutions was 1·1 degK, but in one instance the difference between two successive measurements was as much as 5 degK.

For comparison with the present measurements, the brightness temperatures in two northern regions were calculated by smoothing the observations of PTS and SWCH. The absolute baselevel of the survey of SWCH is based on the same experimental data as those of PTS, and these are not therefore entirely independent sets of data. However, the relative values of brightness temperature are independent in the two studies.

The brightness temperature measured for the northern regions in the present observations and the corresponding temperatures calculated from the data given by PTS and SWCH are given below.

| Region Observed | | Brightness Temperature (°K) | | |
|---|---|---|---|---|
| $\alpha$ | $\delta$ | Present Survey | PTS | SWCH |
| $14^\mathrm{h}\,50^\mathrm{m}$ | $-5°$ | 22·1 | 29·4 | 28 |
| $22^\mathrm{h}\,00^\mathrm{m}$ | $+5°$ | 19·4 | 23·7 | 23 |

The lack of agreement between the present determination of the absolute brightness temperature and that of PTS is obvious. However, not only is there a large difference in the apparent baselevel, but there is a large difference in the relative brightness temperature of the two regions observed. PTS claim that the expected error in the relative value between two regions in their survey is 0·8 degK. The expected errors in the present work for the two northern regions are 3·4 degK.

The difference in level between the two regions in the present measurements is smaller than in the smoothed results of SWCH and PTS. This could be accounted for in the errors of the observations. Considering the differences in the absolute brightness temperatures noted, including the expected errors, we then conclude that the PTS baselevel is too high by some 4–5 degK.

### (c) Second-order Corrections

On the basis of the preceding section it is now possible to estimate the possible errors in $T_\mathrm{s}$ due to an error in the adopted baselevel of the estimated brightness temperature over the sky. A decrease of 4–5 degK as indicated above represents approximately 11% decrease in the contribution to $T_\mathrm{s}$. The value of $T_\mathrm{s}$ decreases from 4·4°K to 4·0°K.

Applying this correction to the values of $\bar{T}_\mathrm{b}$ determined earlier, we obtain the following final brightness temperatures for the regions observed.

| Region Observed | $T_\mathrm{b}$ (°K) | Expected Error (degK) |
|---|---|---|
| South celestial pole | 23·9 | $\pm 1·6$ |
| $\alpha = 14^\mathrm{h}\,40^\mathrm{m},\ \delta = -5°$ | 22·5 | $\pm 3·4$ |
| $\alpha = 22^\mathrm{h}\,00^\mathrm{m},\ \delta = +5°$ | 19·8 | $\pm 3·4$ |

### (d) Expected Errors

The possible sources of error discussed in previous sections are summarized below together with their expected magnitudes. If these errors are independent

of one another, they result in the r.m.s. errors shown above with the final results for brightness temperature.

| Source of Error | R.M.S. Magnitude (degK) |
|---|---|
| Uncertainty in calculated gain of horn | 0·5 |
| Measurement of $T_a$ with respect to termination: | |
|     south celestial pole | 0·4 |
|     northern regions | 3·0 |
| Uncertainty in temperature of reference termination | |
|   contribution due to: | |
|     losses in coaxial section | 0·5 |
|     estimate of temperature of resistive element | 0·5 |
| Temperature scale of noise lamp signal | 0·4 |
| Measurement of losses: horn, waveguide, and matching section | 1·0 |
| Estimate of $T_g$ | 0·5 |
| Estimate of $T_s$ | 0·5 |

## VIII. Acknowledgments

## IX. References

BRAUN, E. H. (1956).—*I.R.E. Trans. Antennas Propag.* **AP4**, 29.

HOGG, D. C. (1959).—*J. appl. Phys.* **30**, 1417.

JULL, E. V., and DELOLI, E. P. (1964).—*I.E.E.E. Trans. Antennas Propag.* **AP12**, 439.

McGEE, R. X., SLEE, O. B., and STANLEY, G. J. (1955).—*Aust. J. Phys.* **8**, 347.

PAULINY-TOTH, I. I. K., and SHAKESHAFT, J. R. (1962).—*Mon. Not. R. astr. Soc.* **124**, 61.

PIDDINGTON, J. H., and TRENT, G. H. (1956).—*Aust. J. Phys.* **9**, 481.

SEEGER, C. L., STUMPERS, F. L. H. M., and VAN HURCH, N. (1960).—*Philips tech. Rev.* **21**, 317.

SEEGER, C. L., WESTERHOUT, G., CONWAY, R. G., and HOEKEMA, T. (1965).—*Bull. astr. Insts Neth.* **18**, 11.

SEEGER, C. L., WESTERHOUT, G., and VAN DE HULST, H. C. (1956).—*Bull. astr. Insts Neth.* **13**, 89.

SILVER, S. (1949).—"Microwave Antenna Theory and Design." M.I.T. Rad. Lab. Series No. 12. (McGraw-Hill: New York.)

SLAYTON, W. T. (1954).—Naval Research Laboratories, Washington, D.C., Rep. No. 4433.

STELZRIED, C. T. (1961).—*Proc. Inst. Radio Engrs* **49**, 1224.